Immunity
Resource

Molecular and Transcriptional Basis of CD4+ T Cell Dysfunction during Chronic Infection

Alison Crawford,[1] Jill M. Angelosanto,[1] Charlly Kao,[1] Travis A. Doering,[1] Pamela M. Odorizzi,[1] Burton E. Barnett,[1] and E. John Wherry[1,*]
[1]Department of Microbiology and Institute for Immunology, Perelman School of Medicine, University of Pennsylvania, Philadelphia, PA 19104, USA
*Correspondence: wherry@mail.med.upenn.edu
http://dx.doi.org/10.1016/j.immuni.2014.01.005

SUMMARY

T cell exhaustion is common during chronic infections. Although CD4+ T cells are critical for controlling viral load during chronic viral infections, less is known about their differentiation and transcriptional program. We defined the phenotypic, functional, and molecular profiles of exhausted CD4+ T cells. Global transcriptional analysis demonstrated a molecular profile distinct from effector and memory CD4+ T cells and also from exhausted CD8+ T cells, though some common features of CD4+ and CD8+ T cell exhaustion were revealed. We have demonstrated unappreciated roles for transcription factors (TFs) including Helios, type I interferon (IFN-I) signaling, and a diverse set of coinhibitory and costimulatory molecules during CD4+ T cell exhaustion. Moreover, the signature of CD4+ T cell exhaustion was found to be distinct from that of other CD4+ T cell lineage subsets and was associated with TF heterogeneity. This study provides a framework for therapeutic interventions targeting exhausted CD4+ T cells.

INTRODUCTION

After acute infections, memory T cells form that persist long term and can rapidly perform effector functions and expand upon reinfection (Jameson and Masopust, 2009). In contrast, during many persisting infections, T cells become "exhausted," a state characterized by poor effector functions and high expression of multiple inhibitory receptors (Wherry, 2011). CD8+ T cell exhaustion occurs in mice during chronic lymphocytic choriomeningitis virus (LCMV) and other chronic infections, in primates infected with simian immunodeficiency virus (SIV), and in humans infected with HIV, hepatitis B virus (HBV), hepatitis C virus (HCV), and other pathogens as well as in humans with cancer (Wherry, 2011). In recent years the pathways involved in CD8+ T cell exhaustion have begun to be defined. In contrast, although CD4+ T cells play a pivotal role in chronic infection and cancer, the effect of persisting infection on their function and differentiation remains less well understood.

Robust and functional CD4+ T cell responses are a critical feature of effective antiviral immunity and can prevent CD8+ T cell exhaustion during chronic viral infections. For example, CD4+ T cell depletion during chronic LCMV infection leads to lifelong uncontrolled viremia (Matloubian et al., 1994). Similarly, during HIV infection, the progression to AIDS is temporally associated with (and defined by) loss of CD4+ T cells. During HCV infection, a robust early CD4+ T cell response is important for clearing the infection and chronic infection is accompanied by low or absent CD4+ T cell responses whereas resolution is associated with vigorous CD4+ T cell responses (Schulze Zur Wiesch et al., 2012).

Although CD4+ T cell production of interferon-γ (IFN-γ), tumor necrosis factor-α (TNF-α), and interleukin-2 (IL-2) is decreased during chronic infection, suggesting similar defects as exhausted CD8+ T cells (Wherry, 2011), other functions such as production of IL-10 and IL-21 are increased (Brooks et al., 2006; Ejrnaes et al., 2006; Elsaesser et al., 2009; Fröhlich et al., 2009). IL-21 is important for CD8+ T cells in this setting, but could also influence B cells. In chronic LCMV and HCV infections, large amounts of T-cell-dependent virus-specific antibodies are produced, suggesting that at least some aspects of CD4+ T cells help B cells remain intact (Bartosch et al., 2003; Buchmeier et al., 1980), and virus-specific CD4+ T cells transferred to chronically infected mice remain capable of providing help to B cells for at least 50 days (Oxenius et al., 1998). Thus, whether CD4+ T cells become exhausted during chronic infection or develop down an alternate path of differentiation remains unclear. Moreover, the extent to which the program of exhaustion of CD4+ and CD8+ T cells overlaps during chronic viral infection is unknown. Together, these studies indicate that although CD4+ T cells develop some functional defects, they may gain and/or sustain other properties during chronic infection, suggesting that the impact of chronic infection on exhaustion of CD4+ and CD8+ T cells might be different.

To begin to define the molecular pathways involved in CD4+ T cell dysfunction during chronic infection, genome-wide transcriptional profiling was performed. A common signature of exhaustion shared between virus-specific CD4+ and CD8+ T cells was revealed, as well as unique aspects of CD4+ T cell exhaustion. CD4+ T cell exhaustion was defined by a distinct pattern of inhibitory and costimulatory molecule expression, cell cycle changes, and a unique TF profile. In addition, exhausted CD4+ T cells showed a loss of a strong T helper 1

(Th1)-cell-associated transcriptional signature but not an obvious skewing toward Th2, Th17, T follicular helper (Tfh), or inducible regulatory T (iTreg) cell fates. These studies provide insights into the molecular mechanisms of $CD4^+$ versus $CD8^+$ T cell dysfunction during chronic infection and define the nature of $CD4^+$ T cell exhaustion versus memory. Specific genes and pathways identified here represent potential therapeutic targets for interventions aimed at restoring function from exhausted $CD4^+$ T cells. Moreover, the broader signatures of $CD4^+$ T cell exhaustion might aid in identifying this type of T cell dysfunction in other settings to predict disease progression or therapeutic efficacy of vaccines or other interventions.

RESULTS

Virus-Specific $CD4^+$ T Cells Have Altered Effector Functions during Chronic Infection

Infection with LCMV Armstrong (Arm) results in an acute infection whereas clone 13 causes a chronic infection (Ahmed et al., 1984; Wherry et al., 2003). To define how chronic infection affects $CD4^+$ T cell differentiation, we examined LCMV-specific $CD4^+$ T cell responses after either Arm or clone 13 infection (Figure 1). LCMV-specific $CD4^+$ T cells underwent robust clonal expansion and persisted long term after Arm or clone 13 infection (Figure 1A), though the magnitude of the response was lower during clone 13 infection.

To compare dysfunction between virus-specific $CD4^+$ and $CD8^+$ T cell responses, we measured IFN-γ, TNF-α, and IL-2 ex vivo by intracellular cytokine staining (ICS). During clone 13 infection, $CD8^+$ T cells initially developed effector functions but became progressively dysfunctional (Figures 1B and 1D, Figure S1 available online; Wherry, 2011). LCMV-specific $CD4^+$ T cells also displayed poor coproduction of cytokines or polyfunctionality after infection with clone 13 (Figures 1C, 1E, and S1; Brooks et al., 2005; Fuller and Zajac, 2003; Oxenius et al., 1998). It was unclear whether this $CD4^+$ T cell dysfunction was progressive, as was the $CD8^+$ T cell response, or arose early during infection. To examine this issue, we compared IFN-γ production/cell as a percentage of that observed on day 6 (d6). These analyses revealed that IFN-γ production by $CD8^+$ T cells gradually waned whereas IFN-γ production by $CD4^+$ T cells changed little from the low production at d6 postinfection (p.i.) (Figures 1F and 1G). Thus, endogenous virus-specific $CD4^+$ T cell responses during clone 13 infection display early and sustained dysfunction compared to memory $CD4^+$ T cells in agreement with previous data with TCR transgenic cells (Brooks et al., 2005).

In contrast, IL-21 expression was higher in exhausted $CD4^+$ T cells (Figure 1H; Elsaesser et al., 2009; Fröhlich et al., 2009; Yi et al., 2009), and a subpopulation of exhausted $CD4^+$ T cells also coproduced IL-10 with IFN-γ (Figure 1I; Brooks et al., 2006). Together these observations indicate that $CD4^+$ T cells do not merely lose cytokine production, but rather have an altered functional profile, suggesting a change in the pattern of differentiation during chronic infection.

Comparing Transcriptional Profiles of $CD4^+$ and $CD8^+$ T Cells from Acute versus Chronic Infection

To examine the molecular mechanisms of altered function of $CD4^+$ T cells during chronic infection, global transcriptional profiling was performed on tetramer$^+$ $CD4^+$ or $CD8^+$ T cells at d8, d15, and d30 p.i. (Figures 2A and 2B). This approach allowed direct comparison of $CD4^+$ and $CD8^+$ T cells from mice with the same viral load. An initial evaluation confirmed changes known to occur in effector, memory, and exhausted T cells (Figure S2; Wherry et al., 2007). Pairwise comparisons of exhausted $CD4^+$ T cells with naive, effector, and memory $CD4^+$ T cells revealed a total of 715 transcripts differentially expressed (>2-fold) in exhausted compared to naive $CD4^+$ T cells (Table S1). To compare the $CD4^+$ T cell responses during clone 13 versus Arm infection over time, we calculated the number of differentially expressed genes unique to $CD4^+$ T cells that responded to either infection. Early in the response (d8), few genes were uniquely changed in either infection, suggesting that, initially, effector $CD4^+$ T cells have a similar transcriptional profile in both infections. However, gene expression of the $CD4^+$ T cells responding to the two infections diverged as the chronic infection evolved (Figure 2C). A similar pattern was observed for $CD8^+$ T cells, suggesting that this divergence was common for both $CD4^+$ and $CD8^+$ T cells.

One possibility was that T cells responding to chronic infection remain in a prolonged effector state. To test this possibility, we compared the differentially expressed genes in $CD4^+$ T cells responding to chronic infection on different days p.i. with those of effector $CD4^+$ T cells on d8 p.i. with Arm. The transcriptional profiles at d15 and d30 p.i. of clone 13 infection were distinct from those of effector cells, suggesting that the $CD4^+$ T cells responding to chronic infection were not simply arrested in an effector state (Figure 2D). A similar pattern was observed with the clone 13 d8 signature as the "denominator" (Figure S2). Indeed, exhausted $CD4^+$ T cells had a distinct transcriptional profile compared to effector and memory $CD4^+$ T cells (Figure 2E). A similar pattern was observed for exhausted $CD8^+$ T cells. Although exhausted $CD4^+$ and $CD8^+$ T cells were distinct from effector and memory T cells of the same lineage, unsupervised hierarchical clustering indicated that whereas exhausted and memory $CD4^+$ T cells were clearly distinct, these cells were more closely related to one another than exhausted $CD4^+$ T cells were to exhausted $CD8^+$ T cells (Figure 2F). Although $CD4^+$ and $CD8^+$ T cells remained as separate branches, within each lineage, samples clustered mainly by time point. Thus, the profile of exhausted $CD4^+$ T cells is divergent from effector and memory $CD4^+$ T cells as well as exhausted $CD8^+$ T cells.

Transcriptional Profiles Reveal Categories of Genes Prominently Associated with Exhausted $CD4^+$ T Cells

To begin to define how cellular processes were impacted in exhausted $CD4^+$ T cells, differentially expressed genes were assigned to putative functional categories (Tables 1 and S2). This analysis revealed categories with substantial (>50%), moderate (35%–50%), or low (<35%) numbers of genes shared between exhausted and memory $CD4^+$ T cells (Table 1). Categories with substantial overlap included metabolism, costimulation, cytokines, chemokines, and adhesion molecules. Categories with moderate overlap included those involved in regulating cell signaling, inhibitory molecules, and transcription. In this set, half of the transcripts had similar changes during chronic and acute infection whereas the remainder was unique to either infection. In this latter group, genes tended to be exhaustion biased. The categories with low overlap included

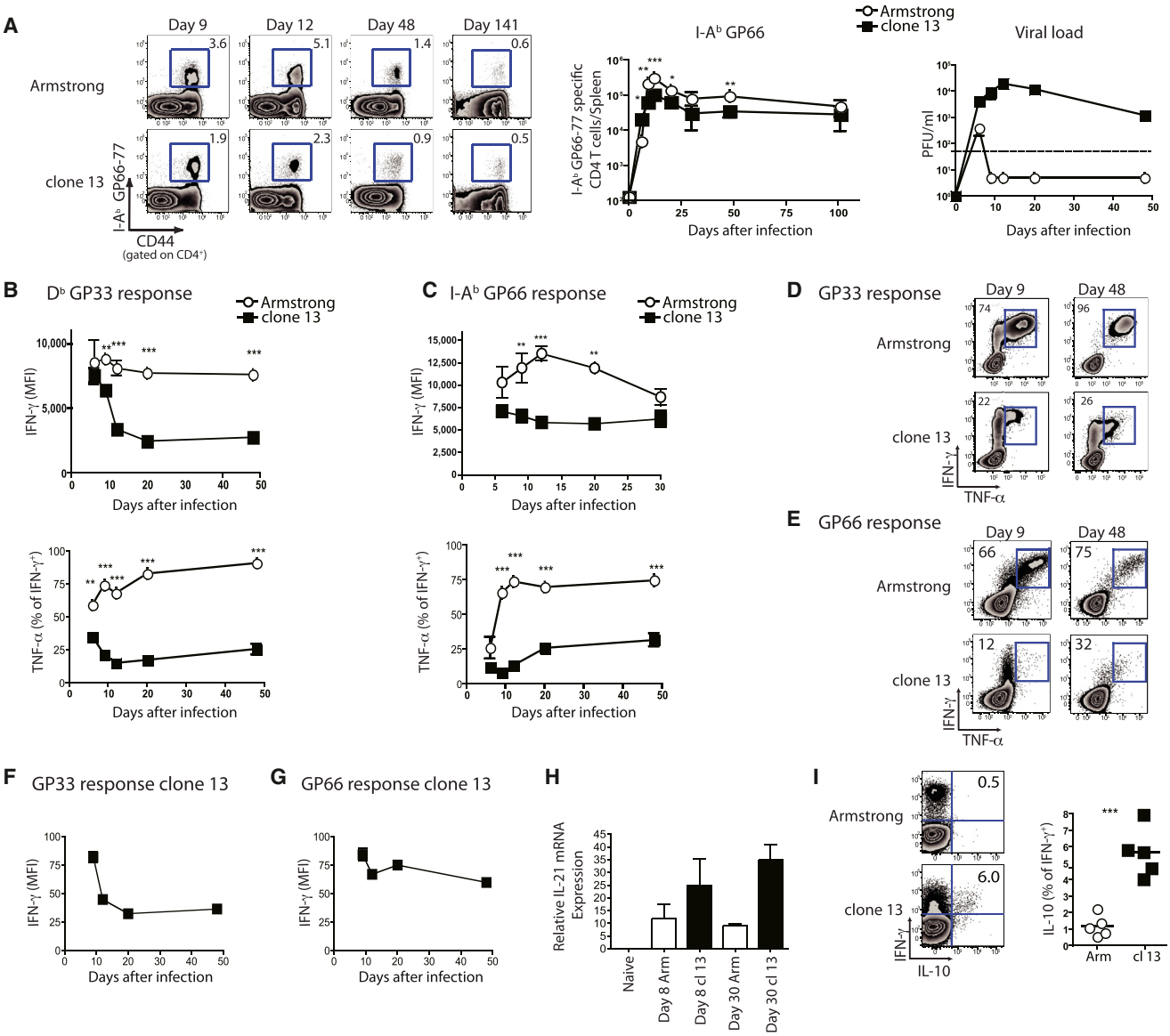

Figure 1. Kinetics of Cytokine Production by Virus-Specific CD4+ and CD8+ T Cells during Chronic LCMV Infection

(A) Representative flow plots of I-A^{b}GP$_{66}$ tetramer staining on the indicated days p.i. with Arm or clone 13. Numbers show percent of CD4+ T cells specific for GP66. Middle: Total number of I-A^{b}GP66 tetramer+ CD4+ T cells in spleen during acute (open symbols) or chronic (closed symbols) LCMV infection. Right: Viral load in the serum over time after infection with either Arm (open symbols) or clone 13 (filled symbols).

(B) MFI of IFN-γ in response to GP33 stimulation (top) and the percentage of IFN-γ-producing cells coproducing TNF-α (bottom).

(C) CD4+ T cell responses to GP$_{66-77}$ as described in (B).

(D and E) Representative flow plots are shown for cytokine coproduction in response to GP33 (D) or GP66 (E) peptide.

(F and G) MFI of IFN-γ as a percentage of d6 IFN-γ MFI for CD8+ (F) and CD4+ (G) T cells.

(H) IL-21 mRNA expression on d8 and d30 p.i. with Arm or clone 13 in sorted I-A^{b}GP66 tetramer+ CD4+ T cells.

(I) Representative plots of IFN-γ and IL-10 production by GP66-specific CD4+ T cells on d30 p.i. and summary of the percent of IFN-γ producers making IL-10.

Data are representative over at least three independent experiments with two to four mice/group. Error bars indicate standard deviation. See also Figure S1.

"IFN-induced" genes and genes involved in cell cycle and DNA repair and remodeling. Regulation of many genes in these categories was biased toward exhausted CD4+ T cells. An exception was the set of genes involved in DNA repair, which was biased toward memory. This analysis identifies potential cellular pathways of interest that distinguish functional memory CD4+ T cells from CD4+ T cells responding to chronic infection.

The IFN-Responsive Pathway Is Associated with CD4+ T Cell Exhaustion

To define additional biological pathways associated with CD4+ T cell exhaustion, we used gene set enrichment analysis (GSEA) and a curated panel of gene sets from the Molecular Signatures Database (MSigDB; the C2 set) that contains information about biological pathways, disease phenotypes, and gene sets

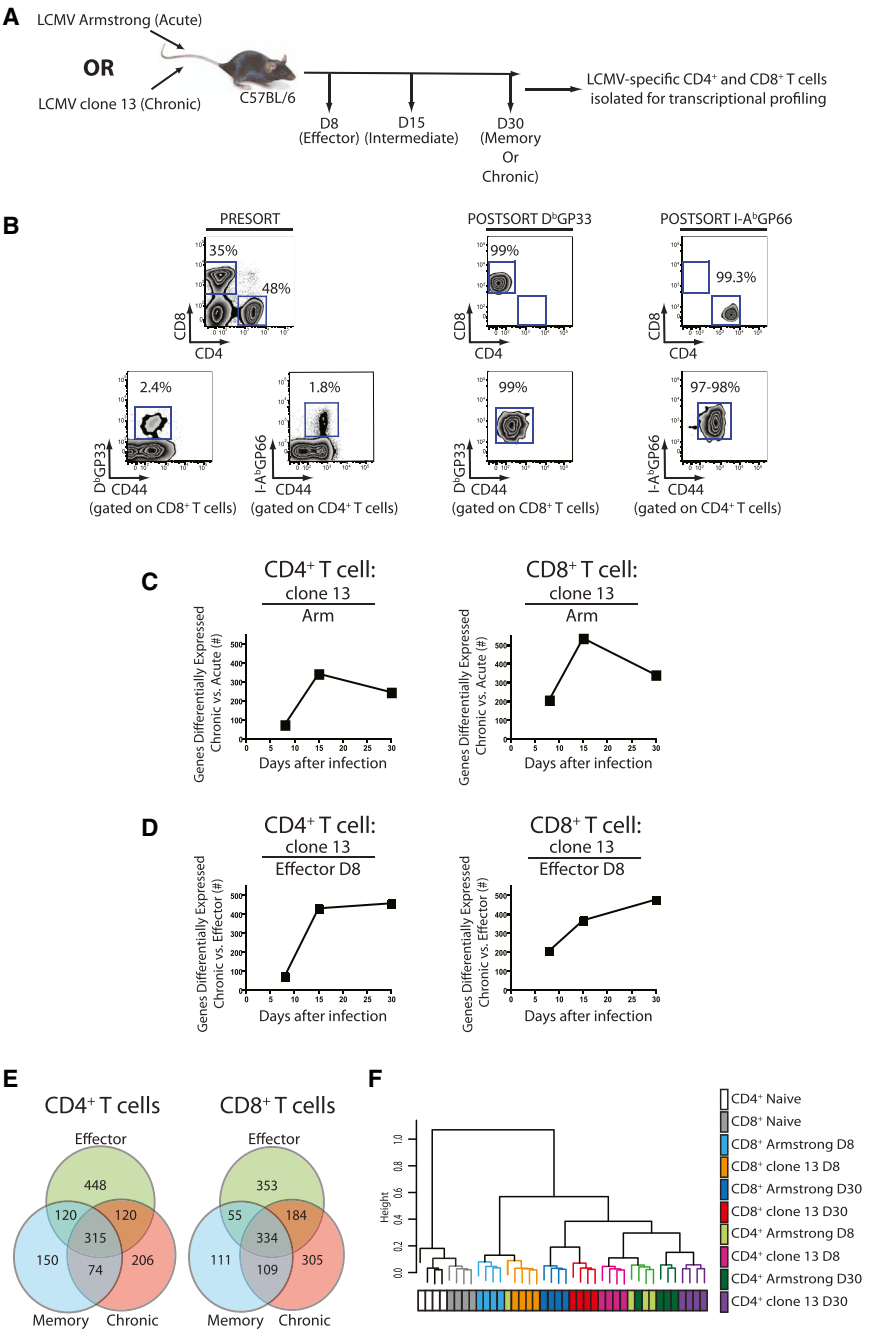

Figure 2. Transcriptional Profiling of LCMV-Specific CD4+ and CD8+ T Cells from Mice Infected with Arm or Clone 13

(A) Schematic of the experimental design.

(B) Presort and postsort purities for D^bGP33-specific $CD8^+$ T cells and I-A^bGP66-specific $CD4^+$ T cells.

(C) The number of differentially expressed genes for $CD4^+$ (left) and $CD8^+$ (right) T cells from clone 13 compared to Arm at each time p.i.

(D) The total number of differentially expressed genes from virus-specific $CD4^+$ or $CD8^+$ T cells from clone 13-infected mice on d8, d15, and d30 p.i. compared to d8 effector T cells from Arm.

(E) Differentially expressed genes between d8 effector T cells from Arm-infected mice, memory T cells from d30 p.i. with Arm, and exhausted T cells isolated from d30 p.i. with clone 13.

(F) Hierarchical clustering of $CD4^+$ and $CD8^+$ T cell responses to acute and chronic infections. Genes differentially expressed by a covariance of 0.1 were analyzed by Spearman's correlation. Microarray data are representative of four independent samples per time point.

See also Figure S2 and Table S1.

from the biomedical literature. Several gene sets enriched in exhausted, compared to effector and memory $CD4^+$ T cells (false discovery rate [FDR] < 0.1), were associated with inflammation including type I IFN (IFN-I) signaling (Figure 3A). We next used a signature of IFN-I-induced transcriptional changes (Agarwal et al., 2009) and GSEA to test whether this biologically defined type I IFN signature was enriched in memory versus exhausted $CD4^+$ or $CD8^+$ T cells. Indeed, both $CD4^+$ and $CD8^+$ T cells from chronically infected mice showed a strong enrichment for type I IFN-induced transcriptional changes (Figure 3B).

The presence of a strong type I IFN signature at d30 of chronic infection was intriguing because circulating type I IFN is not detectable at this time (Lee et al., 2009; Zuniga et al., 2008). Many of the IFN-induced genes upregulated in exhausted $CD4^+$ T cells (Table S2) were also present in the early stages (e.g., d6–d8) of both infections (Figure 3C). As virus was cleared in Arm infection, however, expression of these genes returned to baseline. In contrast, expression of the majority of these genes was high and sustained in T cells responding to clone 13 infection (Figures 3C and S3A). Because circulating type I IFN peaks and resolves with similar kinetics in Arm and clone 13 infections (Lee et al., 2009; Zuniga et al., 2008), these observations suggest a disconnect between detectable circulating type I IFN protein and activation of the downstream IFN-dependent transcriptional programs in $CD4^+$ T cells during acute versus chronic infections.

We next examined phosphorylated signal transducer and activator of transcription-1 (pStat1) directly ex vivo and after stimulation with IFN-β or IFN-γ. Phosphorylated Stat1 was detectable directly ex vivo in total $CD4^+$ T cells from chronically infected mice, but not in $CD4^+$ T cells from Arm-immune mice (Figures S3B and S3C). However, the ability of $CD4^+$ T cells from chronically infected mice to increase pStat1 in response to IFN-I or IFN-γ was blunted compared to the pStat1 induction in $CD4^+$ T cells from Arm-immune mice. These observations suggest that exhausted $CD4^+$ T cells are subjected to ongoing chronic Stat1 activation and desensitization of this pathway or express negative regulators of IFN signaling, such as Socs proteins.

Table 1. Percentage of Differentially Expressed Genes that Are Unique or Shared between CD4+ T Cells from Clone 13- and Armstrong-Infected Mice

Category	Clone 13	Shared	Armstrong
Cytokines/chemokines	6	76	18
Adhesion/integrins	25	75	0
Regulation of apoptosis/cell death	21	73	6
Cytokine receptors/chemokine receptors	26	70	4
Metabolism	32	60	8
Ubiquitin ligase activity/ proteasome	25	58	17
Costimulatory molecules	27	55	18
Vesicle/membrane biology	38	52	10
Cell surface	41	51	8
Coinhibitory molecules	38	50	13
Cell signaling	46	49	5
Regulation of transcription	32	48	20
Solute carriers	27	47	27
Phosphatases	45	45	9
Cytoskeleton	47	35	18
IFN-induced	53	33	13
Antigen receptors/MHC	15	31	54
Regulation of cell proliferation/ cell cycle	60	29	11
DNA repair/replication	21	29	50
RNA binding/ribosomal	29	29	43
DNA structure	59	18	24

Numbers are the percent of total genes in category that are either biased towards CD4+ T cells from clone 13 infection, towards memory CD4+ T cells, or differentially expressed by both (compared to naive T cells).

Of note, Socs1 and Socs3 mRNA was upregulated in CD4+ T cells during clone 13 infection (Figure S3D).

To further investigate pathways similarly regulated in exhausted CD4+ and CD8+ T cells, we analyzed the differentially expressed genes common to exhausted CD4+ and CD8+ T cells (but unchanged in memory T cells) (Table S3) via Ingenuity Pathway Analysis (IPA) (Figure 3D). Three networks were identified (scores > 2 have at least 99% confidence of not being generated by chance). The network with the highest score contained genes involved in antimicrobial responses, inflammatory responses, and cell-to-cell signaling (Figure 3E). This analysis revealed an association of the IFN pathway with transcriptional pathways including NF-κB, NFAT, and Eomesodermin (Eomes), as well as the inhibitory receptor LAG-3 and the adaptor protein SH2D1A (Sap).

Expression of Distinct Patterns of Inhibitory Receptors in Exhausted CD4+ and CD8+ T Cells

A key feature of CD8+ T cell exhaustion is sustained expression of multiple inhibitory receptors (Blackburn et al., 2009). Although virus-specific CD4+ T cells also express inhibitory receptors during chronic infections (reviewed in Odorizzi and Wherry, 2012), it is unclear whether these cells express the same repertoire of inhibitory receptors as do exhausted CD8+ T cells. Both virus-specific CD4+ and CD8+ T cells upregulated inhibitory receptors during clone 13 infection (Figure 4A). However, the specific inhibitory receptors upregulated and the degree of expression differed greatly between CD4+ and CD8+ T cells. Some inhibitory receptor genes were biased toward exhausted CD8+ T cells including *Cd244*, *Havcr2* (encoding Tim3), and *Lilrb4*. Other inhibitory receptors, however, were biased toward expression in CD4+ T cells including *Ctla4*, *Cd200*, and *Btla* (Figures 4A and 4B). Protein expression confirmed the transcriptional profiles, including CD8+ T-cell-biased 2B4 expression, mutual, though slightly CD8+ biased LAG-3 expression, and CD4+ T-cell-biased CTLA-4 (Figures 4C–4E). PD-1 was highly expressed by CD4+ T cells during chronic infection and this high expression was sustained through at least d50 p.i. (Figures 4C, 4D, 4F, and S4 and data not shown), even when PD-1 expression by exhausted CD8+ T cells in the same mice declined (Figure 4F). The expression of BTLA also differed between CD4+ and CD8+ T cells. CD4+ T cells had increased expression of BTLA during clone 13 infection until ~d20 p.i. and then sustained BTLA expression at least as high as naive T cells (Figure 4G). Virus-specific CD8+ T cells, in contrast, expressed lower BTLA and by d30 p.i. these CD8+ T cells had less BTLA than did naive T cells.

Differential Expression of Costimulatory Receptors in Exhausted CD4+ and CD8+ T Cells

Given the expression of inhibitory receptors during chronic infection, one might predict that costimulatory receptors would be downregulated. However, expression of several costimulatory molecule mRNAs was increased in exhausted CD4+ and CD8+ T cells (Figures 5A and 5B). Whereas *Tfnrsf4* (encoding Ox40) and *Icos* were biased toward expression by CD4+ T cells, *Cd80* was clearly biased toward CD8+ T cells (Figure 5B). Protein expression of OX40 and ICOS showed a strong bias toward expression by CD4+ T cells responding to clone 13 infection in the spleen (Figures 5C and 5D) and other tissues (Figure S4). Exhausted CD4+ T cells also expressed higher CD27 by flow cytometry compared to memory CD4+ T cells (Figure 5F). CD28 was the only costimulatory molecule examined that was slightly decreased on both exhausted CD4+ and CD8+ T cells (Figures 5E and 5F). These data suggest that therapies combining inhibitory receptor blockade and costimulatory receptor engagement may be beneficial.

TFs Involved in CD4+ T Cell Exhaustion

Several TFs including Blimp-1, Batf, T-bet, Eomes, and NFAT have been implicated in CD8+ T cell exhaustion during chronic infection (Agnellini et al., 2007; Kao et al., 2011; Paley et al., 2012; Quigley et al., 2010; Shin et al., 2009). The TFs involved in CD4+ T cell dysfunction during chronic infection, however, are poorly understood. Exhausted CD4+ T cells differentially expressed a number of TFs compared to functional memory CD4+ T cells (Figure 6A and Table S2). First, there was a core set of TFs similarly regulated in memory and exhausted compared to naive CD4+ T cells. This set included *Fosb* and *Id2*. In addition, there was a smaller set of TFs whose change in expression was more associated with memory, including *Klf6*, *Jun*, and *Junb*. Finally, there were several TFs such as *Eomes*, *Prdm1* (Blimp-1),

A

Name	FDR	Description
DOANE BREAST CANCER ESR1 UP	0.00	DE in estrogen receptor negative breast cancer
SEKI INFLAMMATORY RESPONSE LPS UP	0.01	LPS/TLR4 signaling in hepatic stellate cells (HSCs)
SEITZ NEOPLASTIC TRANSFORMATION BY 8P DELETION UP	0.01	Tumor-suppressive genes on human chromosome 8
BROWNE HCMV INFECTION 4HR UP	0.02	Up in human diploid fibroblasts 4 hours after hCMV infection
SANA TNF SIGNALING UP	0.02	TNFα signaling in endothelial cells
YAO TEMPORAL RESPONSE TO PROGESTERONE CLUSTER 6	0.06	Response to progesterone injection
OUYANG PROSTATE CANCER PROGRESSION UP	0.06	Up during prostate cancer progression
LI CISPLATIN RESISTANCE UP	0.06	Up in response to cisplatin chemotherapy drug
LIANG SILENCED BY METHYLATION 2	0.07	Down upon treatment with a methylation inhibitor in bladder carcinoma
DAUER STAT3 TARGETS DN	0.07	Down in lung cancer expressing STAT3
IVANOVA HEMATOPOIESIS STEM CELL	0.07	Up in hematopoietic stem cells (HSC) from adult bone marrow and fetal liver
TAKEDA TARGETS OF NUP98 HOXA9 FUSION 3D UP	0.07	Up in hematopoetic cells by expression of NUP98-HOXA9 oncogene
SU PANCREAS	0.07	Up in human pancreas
BROWNE INTERFERON RESPONSIVE GENES	0.08	Up in primary fibroblasts after interferon alpha for 6 h
HINATA NFKB TARGETS KERATINOCYTE UP	0.08	Up in primary keratinocytes by expression of NFκB1 and RELA
CHEN HOXA5 TARGETS 9HR UP	0.09	DE 9 hr after induction of HoxA5 expression in a breast cancer cell line
ZHANG RESPONSE TO IKK INHIBITOR AND TNF UP	0.09	Up in pancreatic cancer cells after treatment with TNF or an IKK inhibitor
DEBIASI APOPTOSIS BY REOVIRUS INFECTION UP	0.09	Up in embryonic kidney cells at 6h, 12h or 24h after infection with reovirus

B

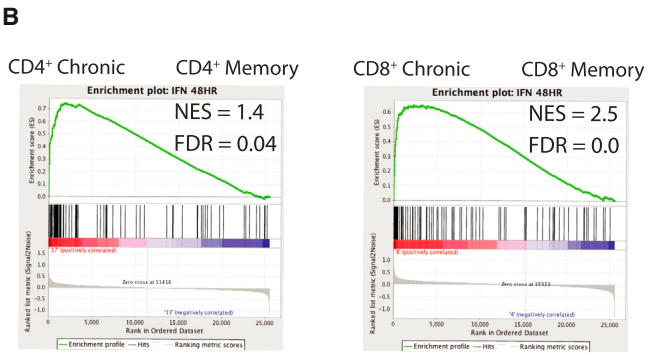

C

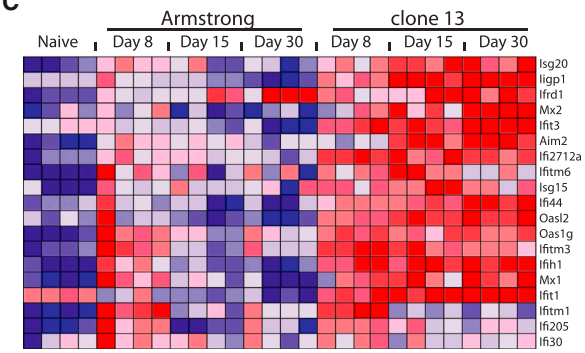

D

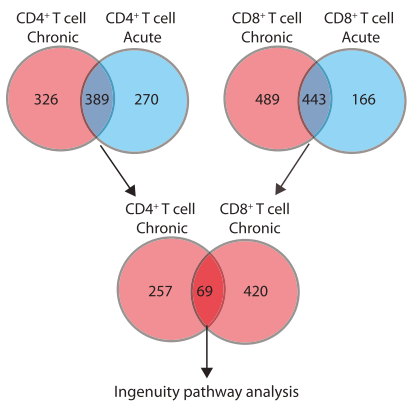

Ingenuity Networks common to both exhausted CD4 and CD8 T cells

Associated Network Functions	Score
Antimicrobial Response, Inflammatory Response, Cell-To-Cell Signaling and Interaction	47
Cellular Assembly and Organization, Cellular Function and Maintenance, Cell Cycle	34
Cell Signaling, Molecular Transport, Small Molecule Biochemistry	27

E

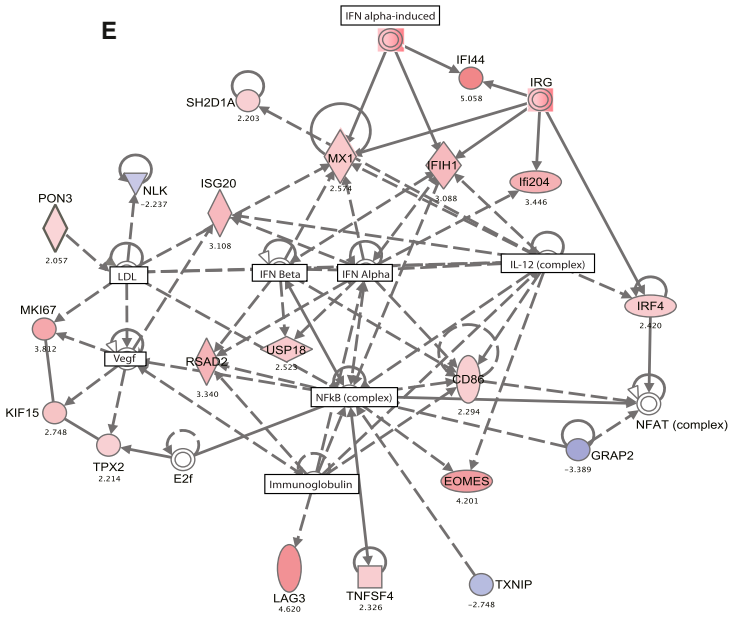

Figure 3. Biological Pathways Enriched in Exhausted CD4+ T Cells

(A) Enriched gene sets in exhausted versus effector or memory CD4+ T cells via GSEA analysis and the MSigDB C2 curated gene sets.

(B) GSEA of exhausted versus memory CD4+ or CD8+ T cells with an IFN-I transcriptional signature (Agarwal et al., 2009).

(C) Heatmap of IFN-responsive genes differentially expressed by exhausted CD4+ T cells (over naive).

(D) The core exhausted signature shared in CD4+ and CD8+ T cells (see also Table S3). Networks identified and their score from Ingenuity pathway analysis are shown.

(E) Ingenuity pathway analysis of the main network associated with both exhausted CD4+ and CD8+ T cells.

See also Figure S3 and Tables S2 and S3.

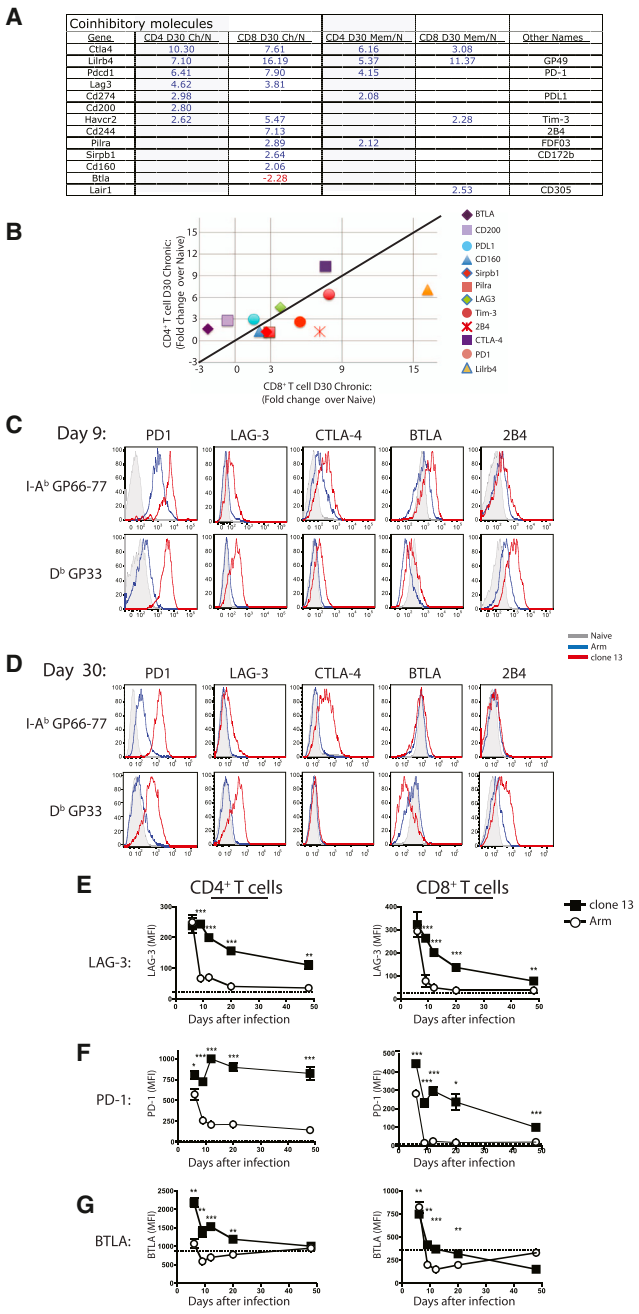

Figure 4. Inhibitory Receptor Expression by Exhausted CD4+ and CD8+ T Cells

(A) Genes encoding coinhibitory receptors differentially expressed by memory and exhausted virus-specific T cells.

(B) Fold change in expression of coinhibitory receptors by exhausted T cells at d30 p.i. compared to naive T cells.

(C and D) Representative histograms showing expression of coinhibitory receptors (PD-1, LAG-3, CTLA-4, BTLA, and 2B4) on LCMV-specific CD4+ and CD8+ T cells on d9 (C) or d30 (D). Histograms depict naive T cells ($CD44^{lo}$; gray) or virus-specific T cells from Arm (blue) or clone 13 (red) infection.

(E–G) MFI of LAG-3 (E), PD-1 (F), and BTLA (G) expression by LCMV-specific CD4+ (left) or CD8+ (right) T cells. Data are representative of three to eight independent experiments with at least three mice per group at each time point. Error bars represent standard deviation.

See also Figure S4 and Table S2.

and *Ikzf2* (Helios) associated with exhausted CD4+ T cells (Figure 6A).

The expression pattern of key transcription factors can, at least partially, define cellular identity and provide clues into the regulation of cellular function and differentiation. We therefore investigated the unique and overlapping TF expression patterns between exhausted CD4+ and CD8+ T cells (Figure 6B). A core set of TFs was changed in a similar manner in virus-specific exhausted CD4+ and CD8+ T cells, including *Batf*, *Tbx21*, *Prdm1*, and *Eomes*. In addition, both exhausted CD4+ and CD8+ T cells had changes for separate sets of TFs. Notable CD8+ T-cell-biased changes in TF expression included downregulation of *Tcf7* whereas CD4+-biased changes included increased *Ikzf2* (Helios) and *Klf4* (Figure 6B). Thus, although there is clearly a core program of T cell dysfunction during chronic infection shared by both lineages, there were also unique transcriptional changes for CD4+ versus CD8+ T cells during chronic infection.

We next examined protein expression for TFs of interest. As expected, T-bet was upregulated upon activation, but its expression was lower in exhausted CD4+ and CD8+ T cells compared to memory T cells (Figure 6C). T-bet is needed to sustain CD8+ T cell responses during chronic infection (Kao et al., 2011; Paley et al., 2012) and T-bet represses PD-1 expression in both CD8+ and CD4+ T cells (Kao et al., 2011). In this regard, it is worth noting that T-bet expression was lower in exhausted CD4+ T cells and PD-1 was higher compared to exhausted CD8+ T cells. We previously demonstrated a role for T-bet in sustaining exhausted CD8+ T cell responses (Kao et al., 2011; Paley et al., 2012). To directly test whether T-bet was required for exhausted CD4+ T cells, we examined LCMV-specific CD4+ T cells during clone 13 infection in WT mice or mice conditionally deficient in one or both copies of *Tbx21* only in T cells (*Tbx21*$^{flox/flox}$*XCd4*^{cre}). In the full (*Tbx21*$^{flox/flox}$*XCd4*^{cre}) or partial (*Tbx21*$^{flox/+}$*XCd4*^{cre}) absence of T-bet there was a significant reduction in the LCMV-specific CD4+ T cells compared to WT mice at d30 p.i. (Figure 6D). T-bet was necessary in a cell-intrinsic manner as indicated by the fact that the tetramer+ response of *Tbx21*$^{-/-}$ CD4+ T cells was substantially lower than that of WT CD4+ T cells in mixed bone marrow chimeras (Figure S5). Thus, although T-bet expression is reduced in CD4+ T cells during LCMV clone 13 infection, low amounts of T-bet are still important to sustain both CD4+ and CD8+ T cell responses during chronic infection.

Eomes is expressed by CD8+ T cells after Arm or clone 13 infection. Although mRNA coding for this TF was not upregulated in effector or memory CD4+ T cells (Figures 6A and 6B and Table S2), *Eomes* was increased in exhausted CD4+ T cells. Flow cytometric analysis revealed expression of Eomes by only a subset of exhausted CD4+ T cells (Figures 6E and 6F). These observations suggest a potential unexpected role for Eomes in CD4+ T cells during chronic viral infection, but also point to heterogeneity in the exhausted CD4+ T cell population (see below).

During clone 13 infection, high Blimp-1 (encoded by *Prdm1*) in CD8+ T cells promotes expression of inhibitory receptors and fosters exhaustion (Shin et al., 2009). *Prdm1* mRNA was also upregulated by exhausted CD4+ T cells. There was again substantial heterogeneity in Blimp-1 expression by flow cytometry (indicated by means of a Blimp-1-YFP reporter) with only a subset of CD4+ T cells expressing high Blimp-1 after Arm or

A

Costimulatory molecules					
Gene	CD4 D30 Ex/N	CD8 D30 Ex/N	CD4 D30 Mem/N	CD8 D30 Mem/N	Other names
Tnfrsf4	7.14		3.01		CD134, Ox40
Icos	6.51	3.12	5.51	3.96	
Cd80	3.89	5.70	2.57	4.72	B7.1
Tnfsf9	3.35	3.07	2.87	2.63	41BBL
Tnfsf4	2.33	3.23			OX40L
Cd86	2.29	2.35			
Tnfsf11	2.02				RANKL
Treml2	-3.71	-4.20	-2.59	-3.17	B7H3
Tnfrsf9		2.13			41BB
Cd40lg			2.25		CD154
CD28			2.18		

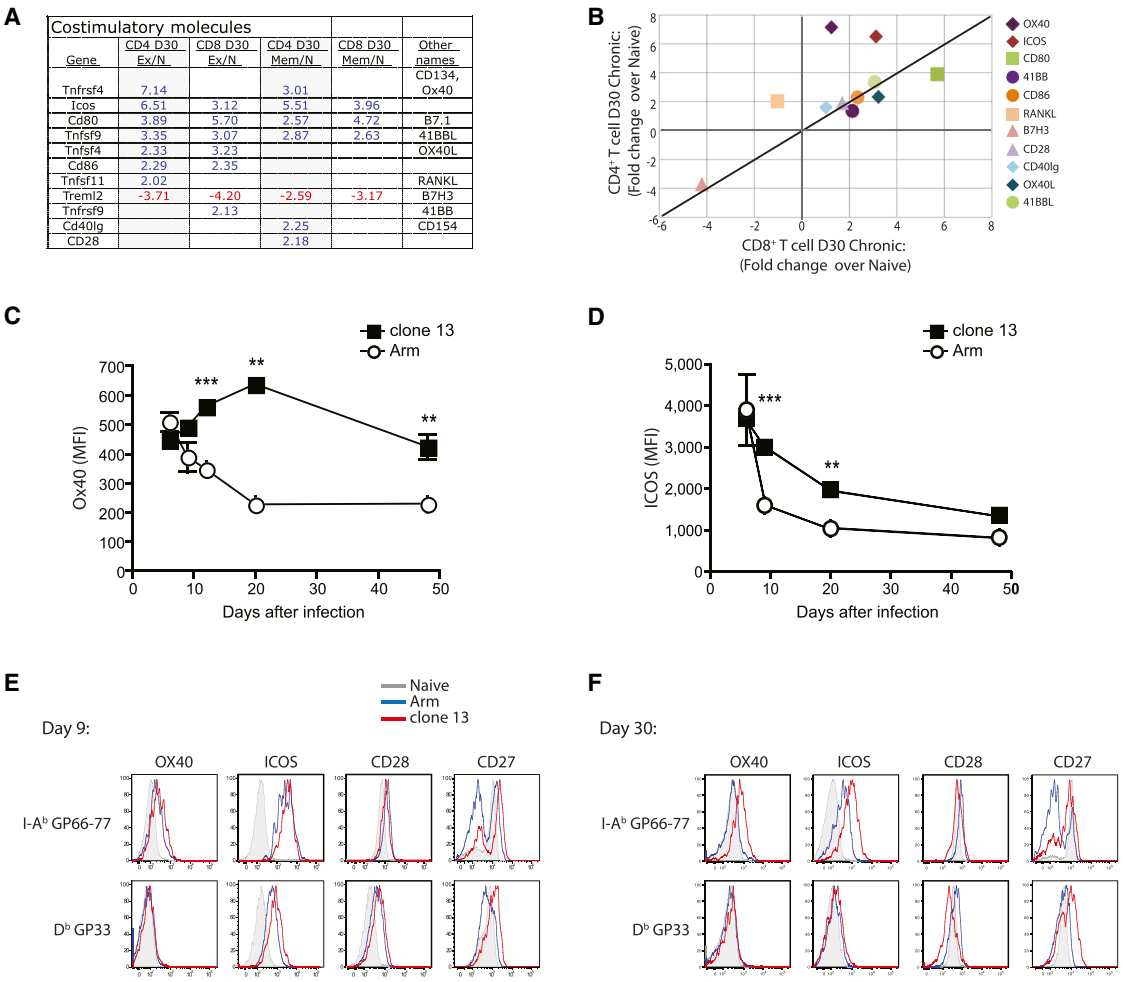

Figure 5. Costimulatory Molecule Expression by T Cells during Arm versus Clone 13 Infection

(A) Genes encoding costimulatory molecules differentially expressed in LCMV-specific CD4+ and CD8+ T cells at d30 p.i.

(B) Fold changes over naive for exhausted CD4+ and CD8+ T cells at d30 p.i.

(C and D) MFI of OX40 (C) and ICOS (D) by I-Ab GP66-specific CD4+ T cells over time.

(E and F) Representative histograms showing expression of ICOS, OX40, CD28, and CD27 at d9 (E) and d30 (F) p.i. Histograms depict naive T cells (CD44lo; gray) or virus-specific T cells from Arm (blue) or clone 13 (red) infection.

Data are representative of four to seven independent experiments with at least three mice per group at each time point. Error bars represent standard deviation. See also Figure S4 and Table S2.

clone 13 infection (Figure 6G). During chronic viral infection, the Blimp-1hi subset of LCMV-specific CD4+ T cells also had high expression of the inhibitory receptor LAG-3 at d30 p.i. (Figure 6H), consistent with observations in exhausted CD8+ T cells (Shin et al., 2009).

The Ikaros family TF Helios (gene *Ikzf2*) was one of the most differentially expressed TFs in exhausted CD4+ T cells compared to memory CD4+ T cells or exhausted CD8+ T cells. During clone 13 infection, virus-specific CD4+ T cells expressed more Helios mRNA and protein than did their effector and memory CD4+ counterparts (Table S2 and Figure 6I). Although Helios is highly expressed by a subpopulation of Treg cells (Getnet et al., 2010), none of the exhausted CD4+ T cells expressed FoxP3 (Figure S5 and see below) and virus-specific CD4+ T cells expressed intermediate amounts of Helios compared to the high amounts in Foxp3+CD4+ T cells (Figure 6J and data not shown). Thus, although both T-bet and Blimp-1 appear to have similar expression patterns in both exhausted CD4+ and CD8+ T cells, other TFs such as Helios are more biased to exhausted CD4+ T cells.

Exhausted CD4+ T Cells Are Heterogeneous and Distinct from Other CD4+ T Cell Effector Subsets

CD4+ T cells can differentiate into distinct lineages including Th1, Th2, Th17, iTreg, and Tfh cells. LCMV Arm infection induces Th1 cells producing IFN-γ. One possible impact of chronic viral infection is skewing of CD4+ T cells to another lineage. Indeed, although no clear signature of lineage-specific TFs was apparent, increased expression of GATA-3 and Bcl6 (Figure 7A) or the cytokines IL-10 and IL-21 (Figure 1) suggested that lineage skewing might occur. The signatures for Th2, Th17, iTreg, nTreg, and Tfh cell subsets and anergic cells defined in previous studies

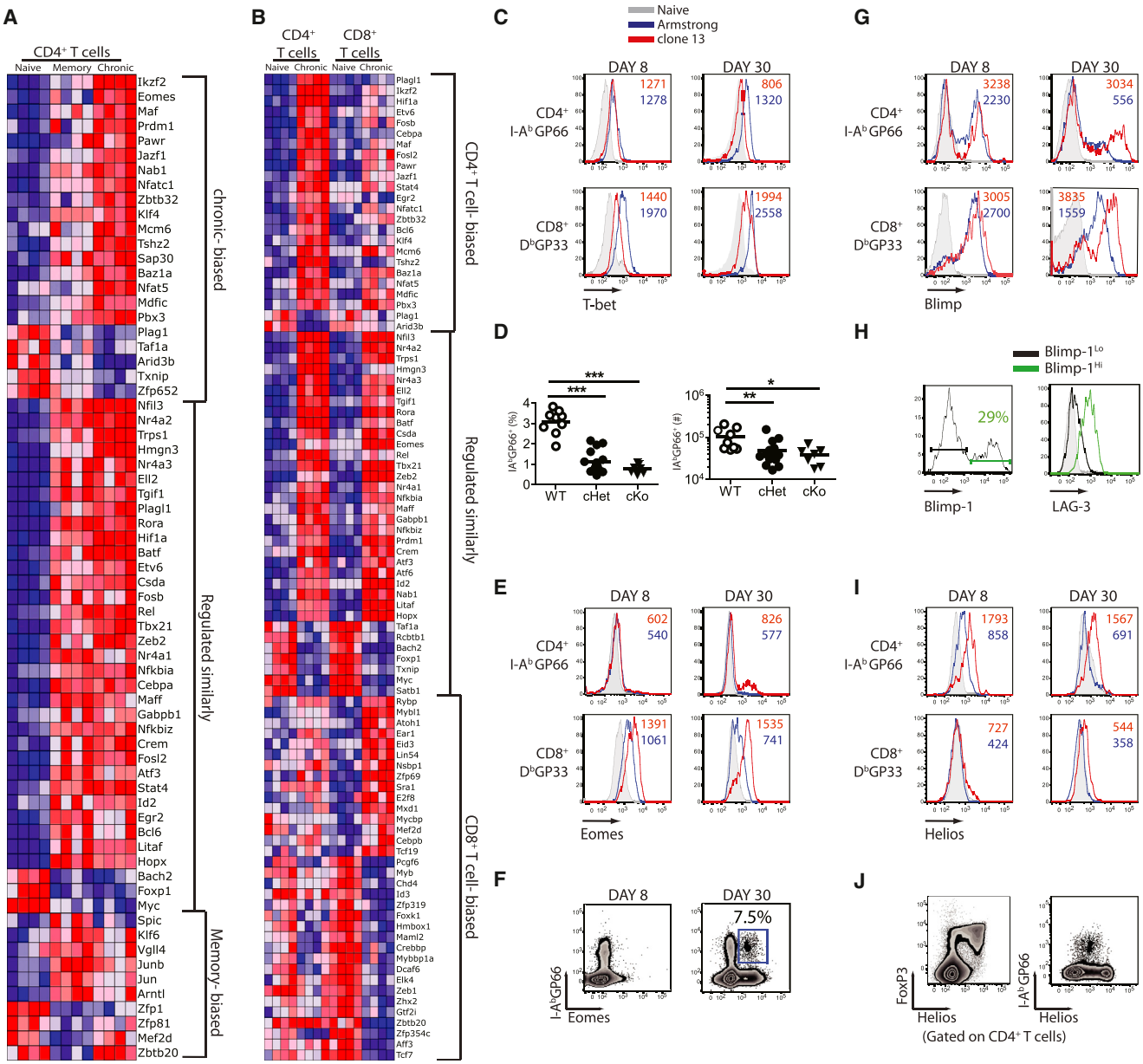

Figure 6. TF Profile of Memory and Exhausted CD4+ and CD8+ T Cells

(A) Heatmap of TFs differentially expressed by either memory or exhausted virus-specific CD4+ T cells.

(B) Heatmap of TFs differentially expressed by exhausted virus-specific CD4+ or CD8+ T cells.

(C) Histograms show protein expression of T-bet by LCMV-specific CD4+ and CD8+ T cells with Arm (blue) or clone 13 (red) infection or in $CD4^+CD44^{lo}$ cells (gray).

(D) I-A^bGP66-specific CD4+ T cell frequency (left) and total numbers per spleen (right) in WT, *Tbx21*$^{flox/+}$*XCd4*^{cre}, or *Tbx21*$^{flox/flox}$*XCd4*^{cre} mice at d30 p.i. with LCMV clone 13.

(E) Eomes expression by LCMV-specific CD4+ and CD8+ T cells from Arm (blue) or clone 13 (red) infection or $CD4^+CD44^{lo}$ cells (gray). Numbers show MFI in cells from clone 13 (red)- or Armstrong (blue)-infected mice.

(F) Representative flow plots for Eomes expression on d8 and d30 p.i. with clone 13. Number shows the percent of I-A^bGP66+ CD4+ T cells expressing Eomes.

(G) Representative histograms of YFP expression by LCMV-specific CD4+ T cells and CD8+ T cells from Blimp-1-YFP reporter mice at d8 and d30 p.i. with LCMV clone 13. Numbers show the MFI of YFP expression in cells from clone 13 (red)- or Armstrong (blue)-infected mice.

(H) At d30 p.i. with clone 13, IA^{b}GP66-specific CD4+ T cells from Blimp-1-YFP mice were gated on Blimp-1^{hi} or Blimp-1^{lo} and examined for LAG-3 expression. Number shows the percent of I-A^bGP66+ CD4+ T cells expressing Blimp-1.

(I) Helios expression by LCMV-specific CD4+ or CD8+ T cells. Gated on I-A^bGP66+ CD4+ T cells from Arm (red) or clone 13 (blue) infection.

(J) Representative flow plots of Helios versus FoxP3 or I-A^bGP66 tetramer for CD4+ T cells at d30 p.i. with clone 13.

Data are representative of two to four independent experiments with at least three mice per group at each time point. See also Figure S5.

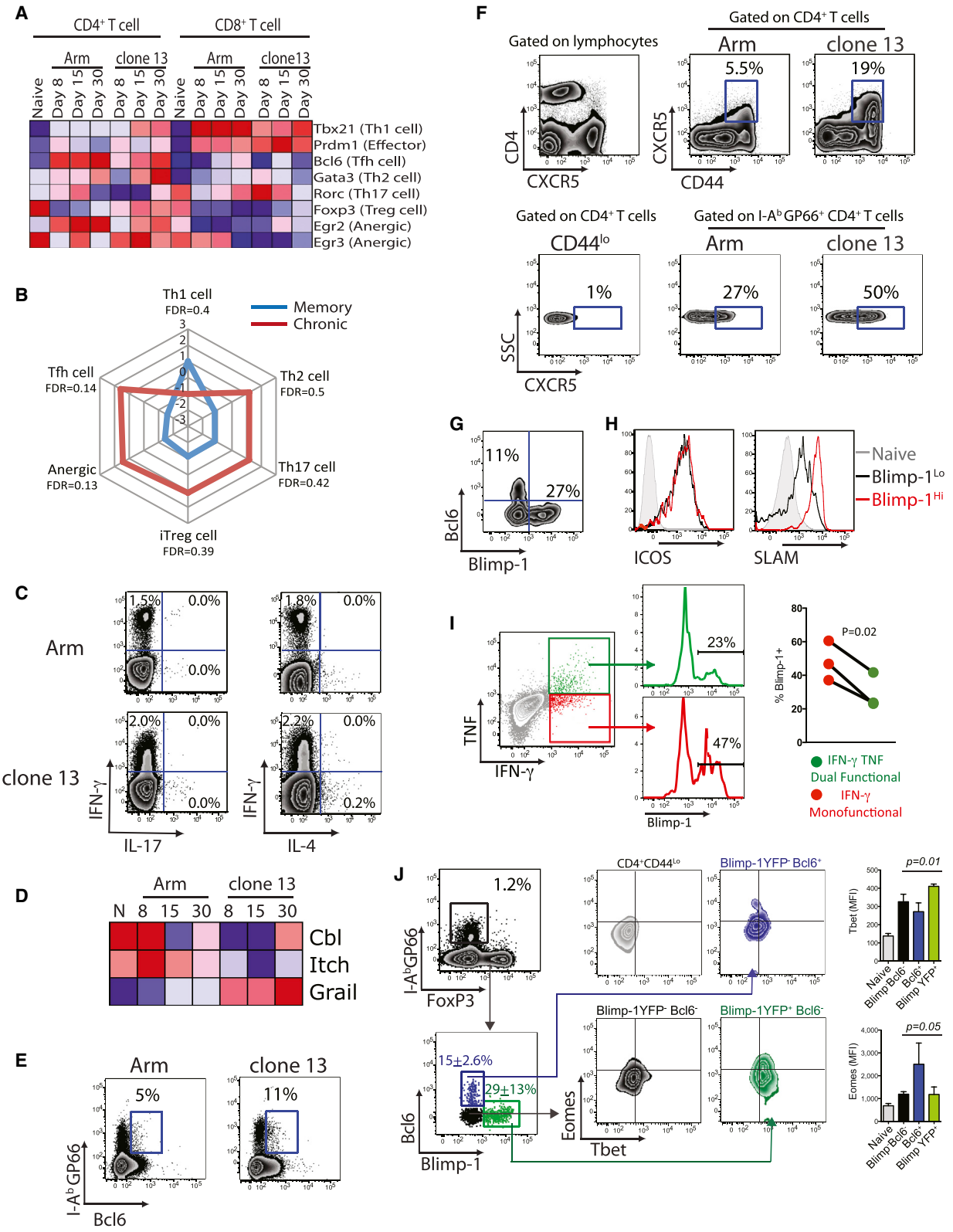

Figure 7. T Helper Cell Lineage Differentiation during Clone 13 Infection

(A) Heatmap of expression of TFs associated with distinct T helper cell lineages in LCMV-specific CD4+ and CD8+ T cells.

(B) GSEA of exhausted versus memory CD4+ T cells with signatures from the specified Th cell subsets. Normalized enrichment scores (NES) are plotted. Red, clone 13; blue, Arm. With an FDR score of 0.01, there was no significant enrichment of any subset for exhausted CD4+ T cells.

(legend continued on next page)

(Safford et al., 2005; Wei et al., 2009; Yusuf et al., 2010) were all slightly biased toward exhausted CD4+ T cells compared to memory CD4+ T cells by GSEA, but no enrichment reached statistical significance (Figure 7B). Indeed, when RT-PCR was used to measure expression of selected TFs, many lineage-defining TFs showed only moderately increased expression in exhausted CD4+ T cell populations compared to memory CD4+ T cells (Figure S6). The major pattern to emerge, however, was the absence of enrichment of a clear Th1 cell signature that was seen for memory CD4+ T cells.

Another possibility was that multiple distinct subpopulations existed during chronic viral infection with each contributing modestly to the transcriptional profile leading to an unfocused enrichment pattern. However, neither IL-4 nor IL-17 protein expression was increased, suggesting that virus-specific CD4+ T cells from chronic infection had not become full-fledged Th2 or Th17 cells (Figure 7C). In addition, essentially all of the I-A^{b}GP66 tetramer+ CD4+ T cells during either Arm or clone 13 infection lacked expression of Foxp3 (Figure S5 and see below). We also examined potential skewing toward anergic T cells or Tfh cells. Anergic CD4+ T cells express ubiquitin protein ligases cbl-b, itch, and GRAIL (Mueller, 2004). Only GRAIL was upregulated by virus-specific CD4+ T cells from chronic infection (Figure 7D). However, GRAIL is also upregulated by Th2 cells from schistosome-infected mice and is required for their hyporesponsiveness (Taylor et al., 2009). Thus, although some molecular components may be shared, CD4+ T cell anergy and CD4+ T cell dysfunction during chronic viral infection may not be entirely overlapping processes.

Recent work suggests a bias toward Tfh cells during chronic viral infections (Fahey et al., 2011). A number of markers have been used to identify Tfh cells including high expression of ICOS, OX40, PD-1, IL-21, CXCR5, Bcl6, and GL7 and low Blimp-1 and SLAM (Johnston et al., 2009). Although several of these markers are also features of exhausted CD4+ T cells (Figures 1 and 6) and might suggest a possible Tfh cell skewing, some can also reflect recent T cell activation. Indeed, although exhausted CD4+ T cells expressed ICOS, OX40, and PD-1, the majority of these cells were Bcl6^{lo} (Figure 7E). We therefore examined the expression of CXCR5 to further investigate the differentiation into Tfh cells. As previously described (Fahey et al., 2011), a higher proportion of LCMV-specific CD4+ T cells isolated from chronically infected mice expressed CXCR5 compared to cells isolated from mice previously infected with LCMV Arm (Figure 7F). Thus, a higher proportion of LCMV-specific CD4+ T cells in chronically infected mice expressed several key Tfh cell markers including CXCR5 and Bcl6. To investigate this issue in more detail, we examined coexpression of Blimp-1 and Bcl6. Consistent with their antagonistic roles (Johnston et al., 2009), the expression of Blimp-1 and Bcl6 in exhausted CD4+ T cells was largely mutually exclusive: Blimp-1^{hi} cells did not express Bcl6 (Figure 7G). SLAM expression was low on some of the Blimp-1^{lo} CD4+ T cells, consistent with a subset of these Blimp-1^{lo} cells expressing Bcl6 (Figure 7H) and representing true Tfh cells. In contrast, both Blimp-1^{lo} and Blimp-1^{hi} cells had high expression of ICOS (Figure 7H), suggesting that ICOS is an unreliable marker of Tfh cells during chronic LCMV infection.

We next investigated whether the heterogeneity in expression of TFs was related to CD4+ T cell function. On d30 p.i., ICS after peptide stimulation revealed IFN-γ and TNF dual cytokine-producing and IFN-γ-producing "monofunctional" populations of virus-specific CD4+ T cells, consistent with Figure 1. To determine whether expression of Blimp-1 was related to CD4+ T cell function, we analyzed YFP expression as a proxy for Blimp-1 in Blimp-1-YFP reporter mice. This analysis demonstrated that virus-specific CD4+ T cells that coproduced IFN-γ and TNF had substantially lower expression of Blimp-1 compared to IFN-γ monofunctional CD4+ T cells that contained an increased proportion of Blimp-1-YFP^{hi} cells. "Reverse" gating also demonstrated that Blimp-1^{hi} cells contained fewer polyfunctional cells than did the Blimp-1^{lo} population (data not shown). These data link TF heterogeneity to function in virus-specific CD4+ T cells from chronic infection and suggest an association between elevated Blimp-1 expression and decreased polyfunctionality. Clearly, however, Blimp-1 expression does not fully account for the full spectrum of heterogeneity in virus-specific CD4+ T cells during chronic infection, and other layers of control (e.g., via other TFs, inhibitory receptors, etc.) are likely to exist.

We next investigated the single-cell coexpression patterns of Blimp-1-YFP, FoxP3, Bcl6, T-bet, and Eomes in exhausted CD4+ T cells on d30 p.i. by flow cytometry (Figure 7J). FoxP3 was not expressed by I-A^{b}GP66-specific CD4+ T cells (Figures 7J and S5). However, three distinct subpopulations were defined by Bcl6 and Blimp-1 expression (Bilmp-1$^+$Bcl6$^-$, Blimp-1$^-$Bcl6$^+$,

(C) Representative flow plots show IL-4 or IL-17 production after peptide stimulation and ICS (gated on CD4+ T cells). Numbers show the percent of CD4+ T cells expressing cytokines.
(D) Heatmap of Cbl, Itch, and Grail expression by LCMV-specific CD4+ T cells.
(E) Representative flow plots of Bcl6 expression by CD4+ T cells at d30 p.i. with Arm or clone 13. Numbers show the percent of I-A^{b}GP66+ CD4+ T cells expressing Bcl6.
(F) CXCR5 expression by total and IA^{b}GP66+ CD4+ T cells. Numbers show the percentage of cells expressing CXCR5.
(G) Representative plots of Blimp-1-YFP versus Bcl6 expression in I-A^{b}GP66+ CD4+ T cells at d30 p.i. with clone 13.
(H) LCMV-specific CD4+ T cells from Blimp-1-YFP mice were examined for expression of ICOS and SLAM at d30 p.i. with clone 13. I-A^{b}GP66+ CD4+ T cells were gated for low or high Blimp-1 expression and then examined for ICOS or SLAM expression.
(I) Blimp-1-YFP mice were infected with LCMV clone 13 and on d30 p.i. ICS was performed with GP66 peptide stimulation followed by staining for IFN-γ and TNF. Dual functional (IFN-γ+TNF+) and monofunctional (IFN-γ+ only) virus-specific CD4+ T cells were then examined for Blimp-1-YFP expression. p value determined by a paired t test.
(J) Representative flow plots of TF expression in I-A^{b}GP66+ CD4+ T cells at d30 p.i. with LCMV clone 13. Foxp3- I-A^{b}GP66+ CD4+ T cells were separated into three distinct populations (Blimp-1$^+$Bcl6$^-$, Blimp-1$^-$Bcl6$^-$, Blimp-1$^+$Bcl6$^+$) and then examined for expression of Eomes and T-bet. Numbers represent the percentage of cells expressing the marker with standard deviation. Statistical relevance was determined by two-way ANOVA.
Data are representative of two to five independent experiments with at least three mice per group at each time point. Error bars represent standard deviation. See also Figure S6.

and Blimp-1^{-}Bcl6^{-}). Within these subsets, T-bet expression was highest in the Blimp-1^{+}Bcl6^{-} subset but was not different between the Blimp-1^{-}Bcl6^{+} and double-negative subsets ($p = 0.01$, two-way ANOVA). In contrast, although some coexpression of Blimp-1 (i.e., YFP) and Eomes was observed, there were also clear populations of Blimp-1^{+}Eomes^{-}, Blimp-1^{-}Eomes^{+}, and double-negative cells (Figures 7J and S6). Thus, virus-specific CD4^{+} T cell populations during chronic LCMV infection were comprised of multiple distinct subsets of cells based on expression of key TFs. Together these studies reveal key insights into the biology of CD4^{+} T cells responding to chronic viral infection. Although there was clearly a shared program with exhausted CD8^{+} T cells such as a signature of ongoing inflammation, CD4^{+} T cells during chronic infection displayed distinct features including an altered profile of inhibitory and costimulatory molecules, a distinct pattern of transcription factor expression, and the existence of multiple distinct subpopulations that may have different function. Future studies are necessary to understand the development and potential to reinvigorate function in these subsets of antiviral CD4^{+} T cells during chronic infection.

DISCUSSION

A major question during chronic infections is whether CD4^{+} and CD8^{+} T cell exhaustion is due to the same molecular pathways. Here we addressed this issue and our results demonstrate that exhausted CD4^{+} T cells differ substantially from effector and memory CD4^{+} T cells. Although there was clearly a core program conserved between exhausted CD4^{+} and CD8^{+} T cells, exhausted CD4^{+} T cells differed in several key respects. We identified cell cycle regulation, DNA repair, IFN-I signaling, altered inhibitory and costimulatory receptor expression, and diverse TF expression patterns among the key changes in exhausted CD4^{+} T cells. TFs and inhibitory receptors are centrally involved in both CD4^{+} and CD8^{+} T cell exhaustion, but the repertoire of inhibitory and transcriptional pathways used was distinct. These data suggest that exhausted CD4^{+} T cells share some transcriptional "modules" with exhausted CD8^{+} T cells but also use other gene expression programs that distinguish them functionally and phenotypically.

We identified a core set of TFs similarly regulated in exhausted CD4^{+} and CD8^{+} T cells. In particular, Blimp-1, T-bet, and Eomes have all been implicated in CD8^{+} T cell responses to infection. Like in CD8^{+} T cells (Shin et al., 2009), high Blimp-1 was associated with increased inhibitory receptor expression and decreased polyfunctionality for exhausted CD4^{+} T cells, though whether Blimp-1 is causal or just associated with these changes will require future investigation. T-bet was also a positive regulator of CD4^{+} T cell responses during chronic LCMV infection, reminiscent of its role in sustaining exhausted CD8^{+} T cells (Kao et al., 2011; Paley et al., 2012). A small subset of exhausted CD4^{+} T cells also expressed Eomes in contrast to lack of this TF in memory CD4^{+} T cells. Finally, the Ikaros family member Helios was strongly biased toward expression in exhausted CD4^{+} T cells. Helios can modulate the function of Ikaros by affecting its intracellular localization (Hahm et al., 1998), perhaps impacting Ikaros-dependent expression of cytokines including IFN-γ, TNF-α, and IL-2 (Quirion et al., 2009). These studies also revealed substantial heterogeneity in TF expression, suggesting that the pool of exhausted CD4^{+} T cells probably represents a mixture of subsets of cells. A single term (exhausted) describing these cells may underrepresent the true diversity of this population. Future studies with TF reporters should allow detailed interrogation of function and lineage relationships between these subpopulations and also facilitate assessment of how expression of individual TFs specifically relates to functional and phenotypic heterogeneity.

Exhausted CD4^{+} and CD8^{+} T cells upregulated IFN-responsive genes during chronic infection, suggesting that T cells were continuing to respond to IFN signals after ~1 month of chronic infection. Serum IFN protein peaks within 48 hr after both Arm and clone 13 infection and falls to baseline within 1 week (Lee et al., 2009; Zuniga et al., 2008), though low IFN mRNA expression has been detected later during chronic LCMV infection (Lee et al., 2009). These observations suggest that exhausted T cells are either able to sustain this IFN-responsive transcription program with minimal continued IFN-I stimulation or that other signals could substitute for IFN-I. Of note, two recent reports demonstrate an immunoregulatory role for type I IFN during chronic LCMV infection and suggest an important role for CD4^{+} T cells in coordinating this effect (Teijaro et al., 2013; Wilson et al., 2013). IFN-responsive genes are also a negative prognostic indicator during human *Mycobacterium tuberculosis* infection (Berry et al., 2010) and are associated with pathogenic SIV infection (Bosinger et al., 2009). Thus, sustained expression of an IFN-I-induced transcriptional program might be a common feature of many chronic diseases, though future studies are necessary to determine the consequences of prolonged expression of this set of genes in CD4^{+} T cells.

Exhausted CD4^{+} T cells also expressed a different repertoire of inhibitory receptors compared to exhausted CD8^{+} T cells. CD4^{+} T-cell-biased expression of inhibitory molecules like BTLA, CTLA-4, CD200, and even PD-1 at later time points, as well as the lack of the CD8^{+} T-cell-biased molecules including 2B4 and Pilra, suggests qualitative differences in the negative regulatory circuits for CD4^{+} and CD8^{+} T cells during the same chronic infection. These differences might reflect ligand availability, different APC interactions, or hardwired transcriptional differences. Surprisingly, with the exception of downregulation of CD28, many costimulatory receptors were increased. Together, these observations suggest that distinct combinations of inhibitory and costimulatory pathways could lead to selective targeting of exhausted CD4^{+} and/or CD8^{+} T cells. Indeed, ligating 4-1BB in combination with blockade of PD-1 leads to a dramatic rescue of exhausted CD8^{+} T cells (Vezys et al., 2011).

During chronic infection, CD4^{+} T cells increased expression of mRNA encoding several TFs implicated in the development of different Th cell subsets including *Tbx21* (Th1 cell), *Gata3* (Th2 cell), *Rora* (Th17 cell), and *Bcl6* (Tfh cell). Although protein expression of some of these TFs was uniform, others such as Blimp-1, Eomes, and Bcl6 were expressed only by subsets of CD4^{+} T cells, suggesting heterogeneity. Blimp-1 and Bcl6 were examined given the expression of a number of Tfh cell-like markers by exhausted CD4^{+} T cells. Bcl6 was expressed by only a subset of these CD4^{+} T cells and this expression was inversely related to Blimp-1. Although Bcl6 staining can be challenging in T cells, combined analyses with Blimp-1 and

CXCR5 expression suggest that it is unlikely that all LCMV-specific CD4+ T cells become true germinal center Tfh cells during chronic infection despite uniformly high expression of some Tfh cell markers like ICOS, OX40, and PD-1. Moreover, the exhausted CD4+ T cells population contained at least partially nonoverlapping subsets of Bcl6+, Blimp-1+, and Eomes+ cells. This observation is consistent with GSEA that demonstrated little enrichment for alternative lineage profiles and suggests a model where exhausted CD4+ T cell populations are heterogeneous, containing multiple distinct subpopulations based on expression of key TFs. Future studies should help clarify precisely how these TF-defined subsets relate to the phenotypic and functional diversity of virus-specific CD4+ T cells during chronic infection.

In summary, this work reveals pathways associated with CD4+ T cell exhaustion and suggests new approaches for therapeutic interventions. The altered pathways identified in CD4+ T cells from chronic infection not only allowed us to gain insight into the unique differentiation of exhausted CD4+ T cells but also revealed shared regulators with exhausted CD8+ T cells. The coinhibitory, costimulatory, inflammatory, and transcriptional pathways identified suggest that exhausted CD4+ and CD8+ T cell subsets are subject to different molecular control and suggest that these T cell populations could be selectively targeted therapeutically.

EXPERIMENTAL PROCEDURES

Animals and Viruses

C57BL/6J mice were purchased from Jackson Laboratories. *Tbx21*^{flox} mice were crossed with *Cd4*^{Cre} mice (Kao et al., 2011). Blimp-1^{YFP} reporter mice were from E. Meffre (Yale University, New Haven, CT). All mice were used in accordance with Institutional Animal Care and Use Committee (IACUC) guidelines. LCMV Arm and LCMV clone 13 were grown in BHK cells and titered on Vero cells (Wherry et al., 2003). Mice were infected with either Arm (2×10^5 PFU) i.p. or clone 13 (2×10^6 PFU) i.v.

Flow Cytometry, Sorting, and Intracellular Cytokine Staining

Lymphocytes were isolated from spleen, stained, and analyzed by flow cytometry as described (Wherry et al., 2003). Virus-specific CD8+ or CD4+ T cells were examined with MHC class I or class II tetramers. MHC class I peptide tetramers were made and used as described (Wherry et al., 2003). MHC class II tetramer was obtained from the NIH Tetramer Core Facility (Emory University, Atlanta, GA). For a list of antibodies used, see Supplemental Experimental Procedures. For ICS, 10^6 splenocytes were cultured in the presence or absence of peptide (0.2 μg/ml for CD8+ peptides and 2 μg/ml for the CD4+ peptide) and brefeldin A for 5 hr at 37°C. Staining was carried out with the BD cytofix/cytoperm kit. Samples were collected by an LSR II flow cytometer (BD).

Gene Expression Profiling

Microarray analysis was performed on four independent samples of FACS-purified T cells from the spleen, sorted based on CD8, CD4, CD44, and tetramer. Cells were sorted directly into TRIzol LS (Invitrogen) and samples were processed and hybridized at the University of Pennsylvania microarray facility with Affymetrix mouse Gene 1.0 ST arrays. Quality-control checks were performed with R (BioConductor). The data were preprocessed with RMA (Robust Multichip Average) normalization. Technical replicates were averaged for fold-change. Genes were considered differentially expressed if they were >2-fold different.

Molecular Signatures and Gene Set Enrichment Analysis

Molecular signatures were generated via the class neighbors function in GenePattern. Genes were ranked with the signal-to-noise ratio (SNR) and a permutation test was used to calculate statistical significance. Gene set enrichment analysis (GSEA) was performed with the Broad Institute program (http://www.broadinstitute.org/gsea/index.jsp). GSEA used gene sets from the Molecular Signature Database v.2.5 (Subramanian et al., 2005) or published gene expression arrays for Th17, iTreg, Th1, and Th2 cells (Wei et al., 2009), anergic T cells (Safford et al., 2005), and Tfh cells (Yusuf et al., 2010). Normalized enrichment score (NES) and q value were calculated by permutation testing.

Statistical Analysis

Nonarray data were analyzed by a two-tailed Student's t test. p value of ≤ 0.05 was considered significant.

ACCESSION NUMBERS

The microarray data are available in the Gene Expression Omnibus (GEO) database (http://www.ncbi.nlm.nih.gov/gds) under the accession number GSE41870, GSE30431, and GSE41867.

SUPPLEMENTAL INFORMATION

Supplemental Information includes Supplemental Experimental Procedures, seven figures, and three tables and can be found with this article online at http://dx.doi.org/10.1016/j.immuni.2014.01.005.

ACKNOWLEDGMENTS

We thank J. Faust, D.J. Hussey, and D.E. Ambrose for FACS sorting. Thanks to members of the E.J.W. lab, G. Perona-Wright, and I. Stylianou for reading of the manuscript. This work was supported by grants from the NIH (AI071309, AI083022, AI082630, AI095608, AI078897, and HHSN266200500030C) to E.J.W. and the American Heart Association postdoctoral fellowship (to A.C.).

Received: June 13, 2013
Accepted: January 2, 2014
Published: February 13, 2014

REFERENCES

Agarwal, P., Raghavan, A., Nandiwada, S.L., Curtsinger, J.M., Bohjanen, P.R., Mueller, D.L., and Mescher, M.F. (2009). Gene regulation and chromatin remodeling by IL-12 and type I IFN in programming for CD8 T cell effector function and memory. J. Immunol. *183*, 1695–1704.

Agnellini, P., Wolint, P., Rehr, M., Cahenzli, J., Karrer, U., and Oxenius, A. (2007). Impaired NFAT nuclear translocation results in split exhaustion of virus-specific CD8+ T cell functions during chronic viral infection. Proc. Natl. Acad. Sci. USA *104*, 4565–4570.

Ahmed, R., Salmi, A., Butler, L.D., Chiller, J.M., and Oldstone, M.B. (1984). Selection of genetic variants of lymphocytic choriomeningitis virus in spleens of persistently infected mice. Role in suppression of cytotoxic T lymphocyte response and viral persistence. J. Exp. Med. *160*, 521–540.

Bartosch, B., Bukh, J., Meunier, J.C., Granier, C., Engle, R.E., Blackwelder, W.C., Emerson, S.U., Cosset, F.L., and Purcell, R.H. (2003). In vitro assay for neutralizing antibody to hepatitis C virus: evidence for broadly conserved neutralization epitopes. Proc. Natl. Acad. Sci. USA *100*, 14199–14204.

Berry, M.P., Graham, C.M., McNab, F.W., Xu, Z., Bloch, S.A., Oni, T., Wilkinson, K.A., Banchereau, R., Skinner, J., Wilkinson, R.J., et al. (2010). An interferon-inducible neutrophil-driven blood transcriptional signature in human tuberculosis. Nature *466*, 973–977.

Blackburn, S.D., Shin, H., Haining, W.N., Zou, T., Workman, C.J., Polley, A., Betts, M.R., Freeman, G.J., Vignali, D.A., and Wherry, E.J. (2009). Coregulation of CD8+ T cell exhaustion by multiple inhibitory receptors during chronic viral infection. Nat. Immunol. *10*, 29–37.

Bosinger, S.E., Li, Q., Gordon, S.N., Klatt, N.R., Duan, L., Xu, L., Francella, N., Sidahmed, A., Smith, A.J., Cramer, E.M., et al. (2009). Global genomic analysis reveals rapid control of a robust innate response in SIV-infected sooty mangabeys. J. Clin. Invest. *119*, 3556–3572.

Brooks, D.G., Teyton, L., Oldstone, M.B., and McGavern, D.B. (2005). Intrinsic functional dysregulation of CD4 T cells occurs rapidly following persistent viral infection. J. Virol. *79*, 10514–10527.

Brooks, D.G., Trifilo, M.J., Edelmann, K.H., Teyton, L., McGavern, D.B., and Oldstone, M.B. (2006). Interleukin-10 determines viral clearance or persistence in vivo. Nat. Med. *12*, 1301–1309.

Buchmeier, M.J., Welsh, R.M., Dutko, F.J., and Oldstone, M.B. (1980). The virology and immunobiology of lymphocytic choriomeningitis virus infection. Adv. Immunol. *30*, 275–331.

Ejrnaes, M., Filippi, C.M., Martinic, M.M., Ling, E.M., Togher, L.M., Crotty, S., and von Herrath, M.G. (2006). Resolution of a chronic viral infection after interleukin-10 receptor blockade. J. Exp. Med. *203*, 2461–2472.

Elsaesser, H., Sauer, K., and Brooks, D.G. (2009). IL-21 is required to control chronic viral infection. Science *324*, 1569–1572.

Fahey, L.M., Wilson, E.B., Elsaesser, H., Fistonich, C.D., McGavern, D.B., and Brooks, D.G. (2011). Viral persistence redirects CD4 T cell differentiation toward T follicular helper cells. J. Exp. Med. *208*, 987–999.

Fröhlich, A., Kisielow, J., Schmitz, I., Freigang, S., Shamshiev, A.T., Weber, J., Marsland, B.J., Oxenius, A., and Kopf, M. (2009). IL-21R on T cells is critical for sustained functionality and control of chronic viral infection. Science *324*, 1576–1580.

Fuller, M.J., and Zajac, A.J. (2003). Ablation of CD8 and CD4 T cell responses by high viral loads. J. Immunol. *170*, 477–486.

Getnet, D., Grosso, J.F., Goldberg, M.V., Harris, T.J., Yen, H.R., Bruno, T.C., Durham, N.M., Hipkiss, E.L., Pyle, K.J., Wada, S., et al. (2010). A role for the transcription factor Helios in human CD4(+)CD25(+) regulatory T cells. Mol. Immunol. *47*, 1595–1600.

Hahm, K., Cobb, B.S., McCarty, A.S., Brown, K.E., Klug, C.A., Lee, R., Akashi, K., Weissman, I.L., Fisher, A.G., and Smale, S.T. (1998). Helios, a T cell-restricted Ikaros family member that quantitatively associates with Ikaros at centromeric heterochromatin. Genes Dev. *12*, 782–796.

Jameson, S.C., and Masopust, D. (2009). Diversity in T cell memory: an embarrassment of riches. Immunity *31*, 859–871.

Johnston, R.J., Poholek, A.C., DiToro, D., Yusuf, I., Eto, D., Barnett, B., Dent, A.L., Craft, J., and Crotty, S. (2009). Bcl6 and Blimp-1 are reciprocal and antagonistic regulators of T follicular helper cell differentiation. Science *325*, 1006–1010.

Kao, C., Oestreich, K.J., Paley, M.A., Crawford, A., Angelosanto, J.M., Ali, M.A., Intlekofer, A.M., Boss, J.M., Reiner, S.L., Weinmann, A.S., and Wherry, E.J. (2011). Transcription factor T-bet represses expression of the inhibitory receptor PD-1 and sustains virus-specific CD8+ T cell responses during chronic infection. Nat. Immunol. *12*, 663–671.

Lee, L.N., Burke, S., Montoya, M., and Borrow, P. (2009). Multiple mechanisms contribute to impairment of type 1 interferon production during chronic lymphocytic choriomeningitis virus infection of mice. J. Immunol. *182*, 7178–7189.

Matloubian, M., Concepcion, R.J., and Ahmed, R. (1994). CD4+ T cells are required to sustain CD8+ cytotoxic T-cell responses during chronic viral infection. J. Virol. *68*, 8056–8063.

Mueller, D.L. (2004). E3 ubiquitin ligases as T cell anergy factors. Nat. Immunol. *5*, 883–890.

Odorizzi, P.M., and Wherry, E.J. (2012). Inhibitory receptors on lymphocytes: insights from infections. J. Immunol. *188*, 2957–2965.

Oxenius, A., Zinkernagel, R.M., and Hengartner, H. (1998). Comparison of activation versus induction of unresponsiveness of virus-specific CD4+ and CD8+ T cells upon acute versus persistent viral infection. Immunity *9*, 449–457.

Paley, M.A., Kroy, D.C., Odorizzi, P.M., Johnnidis, J.B., Dolfi, D.V., Barnett, B.E., Bikoff, E.K., Robertson, E.J., Lauer, G.M., Reiner, S.L., and Wherry, E.J. (2012). Progenitor and terminal subsets of CD8+ T cells cooperate to contain chronic viral infection. Science *338*, 1220–1225.

Quigley, M., Pereyra, F., Nilsson, B., Porichis, F., Fonseca, C., Eichbaum, Q., Julg, B., Jesneck, J.L., Brosnahan, K., Imam, S., et al. (2010). Transcriptional analysis of HIV-specific CD8+ T cells shows that PD-1 inhibits T cell function by upregulating BATF. Nat. Med. *16*, 1147–1151.

Quirion, M.R., Gregory, G.D., Umetsu, S.E., Winandy, S., and Brown, M.A. (2009). Cutting edge: Ikaros is a regulator of Th2 cell differentiation. J. Immunol. *182*, 741–745.

Safford, M., Collins, S., Lutz, M.A., Allen, A., Huang, C.T., Kowalski, J., Blackford, A., Horton, M.R., Drake, C., Schwartz, R.H., and Powell, J.D. (2005). Egr-2 and Egr-3 are negative regulators of T cell activation. Nat. Immunol. *6*, 472–480.

Schulze Zur Wiesch, J., Ciuffreda, D., Lewis-Ximenez, L., Kasprowicz, V., Nolan, B.E., Streeck, H., Aneja, J., Reyor, L.L., Allen, T.M., Lohse, A.W., et al. (2012). Broadly directed virus-specific CD4+ T cell responses are primed during acute hepatitis C infection, but rapidly disappear from human blood with viral persistence. J. Exp. Med. *209*, 61–75.

Shin, H., Blackburn, S.D., Intlekofer, A.M., Kao, C., Angelosanto, J.M., Reiner, S.L., and Wherry, E.J. (2009). A role for the transcriptional repressor Blimp-1 in CD8(+) T cell exhaustion during chronic viral infection. Immunity *31*, 309–320.

Subramanian, A., Tamayo, P., Mootha, V.K., Mukherjee, S., Ebert, B.L., Gillette, M.A., Paulovich, A., Pomeroy, S.L., Golub, T.R., Lander, E.S., and Mesirov, J.P. (2005). Gene set enrichment analysis: a knowledge-based approach for interpreting genome-wide expression profiles. Proc. Natl. Acad. Sci. USA *102*, 15545–15550.

Taylor, J.J., Krawczyk, C.M., Mohrs, M., and Pearce, E.J. (2009). Th2 cell hyporesponsiveness during chronic murine schistosomiasis is cell intrinsic and linked to GRAIL expression. J. Clin. Invest. *119*, 1019–1028.

Teijaro, J.R., Ng, C., Lee, A.M., Sullivan, B.M., Sheehan, K.C., Welch, M., Schreiber, R.D., de la Torre, J.C., and Oldstone, M.B. (2013). Persistent LCMV infection is controlled by blockade of type I interferon signaling. Science *340*, 207–211.

Vezys, V., Penaloza-MacMaster, P., Barber, D.L., Ha, S.J., Konieczny, B., Freeman, G.J., Mittler, R.S., and Ahmed, R. (2011). 4-1BB signaling synergizes with programmed death ligand 1 blockade to augment CD8 T cell responses during chronic viral infection. J. Immunol. *187*, 1634–1642.

Wei, G., Wei, L., Zhu, J., Zang, C., Hu-Li, J., Yao, Z., Cui, K., Kanno, Y., Roh, T.Y., Watford, W.T., et al. (2009). Global mapping of H3K4me3 and H3K27me3 reveals specificity and plasticity in lineage fate determination of differentiating CD4+ T cells. Immunity *30*, 155–167.

Wherry, E.J. (2011). T cell exhaustion. Nat. Immunol. *12*, 492–499.

Wherry, E.J., Blattman, J.N., Murali-Krishna, K., van der Most, R., and Ahmed, R. (2003). Viral persistence alters CD8 T-cell immunodominance and tissue distribution and results in distinct stages of functional impairment. J. Virol. *77*, 4911–4927.

Wherry, E.J., Ha, S.J., Kaech, S.M., Haining, W.N., Sarkar, S., Kalia, V., Subramaniam, S., Blattman, J.N., Barber, D.L., and Ahmed, R. (2007). Molecular signature of CD8+ T cell exhaustion during chronic viral infection. Immunity *27*, 670–684.

Wilson, E.B., Yamada, D.H., Elsaesser, H., Herskovitz, J., Deng, J., Cheng, G., Aronow, B.J., Karp, C.L., and Brooks, D.G. (2013). Blockade of chronic type I interferon signaling to control persistent LCMV infection. Science *340*, 202–207.

Yi, J.S., Du, M., and Zajac, A.J. (2009). A vital role for interleukin-21 in the control of a chronic viral infection. Science *324*, 1572–1576.

Yusuf, I., Kageyama, R., Monticelli, L., Johnston, R.J., Ditoro, D., Hansen, K., Barnett, B., and Crotty, S. (2010). Germinal center T follicular helper cell IL-4 production is dependent on signaling lymphocytic activation molecule receptor (CD150). J. Immunol. *185*, 190–202.

Zuniga, E.I., Liou, L.Y., Mack, L., Mendoza, M., and Oldstone, M.B. (2008). Persistent virus infection inhibits type I interferon production by plasmacytoid dendritic cells to facilitate opportunistic infections. Cell Host Microbe *4*, 374–386.